CrystEngComm

COMMUNICATION

View Article Online
View Journal | View Issue

Solid-state coexistence of $\{Zr_{12}\}$ and $\{Zr_6\}$ zirconium oxocarboxylate clusters†

Cite this: *CrystEngComm*, 2014, **16**, 43

Received 10th September 2013,
Accepted 30th October 2013

DOI: 10.1039/c3ce41829d

www.rsc.org/crystengcomm

Iurie L. Malaestean,[a] Meliha Kutluca Alıcı,[a] Claire Besson,[a] Arkady Ellern[b] and Paul Kögerler*[a]

Ligand metathesis, Co(II) coordination, and partial condensation reactions of an archetypal $\{Zr_6\}$ zirconium oxocarboxylate cluster result in the first example of the coexistence of the distinct zirconium oxide frameworks $\{Zr_6O_8\}$ and $\{Zr_{12}O_{22}\}$. Even minor modifications to the reaction conditions push this apparent equilibrium towards the $\{Zr_6O_8\}$-based product.

Molecular high-nuclearity zirconium(IV) and cerium(III/IV) oxide structures have emerged as an extension to classical polyoxometalate chemistry with numerous structural analogies and similar formation paradigms.[1] In this context, we have explored the magnetic functionalization of several zirconium(IV) oxide clusters based on highly condensed $\{Zr_6O_8\}$[2] and $\{Zr_{12}O_{22}\}$[3] frameworks. Whereas little is known about the equilibria of different structural zirconium oxide archetypes in their reaction solutions, their similarity to group-5/6 polyoxometalates, where numerous species or isomers commonly coexist, suggests that, under certain boundary reaction conditions, different zirconium oxide structures could coexist as well. We now scanned the reaction parameter space for Co(II)-substituted zirconium oxocarboxylate clusters, starting from a member of the well-established $\{Zr_6O_4(OH)_4(carboxylate)_{12}\}_2$-type cluster family of clusters, namely $[Zr_6O_4(OH)_4(pr)_{12}]$ (pr: propionate). Reactions were performed in the presence of potential bridging ligands in acetonitrile and small, well-defined amounts of water that facilitate further hydrolysis or condensation steps.‡ This approach yielded a crystalline phase of composition $\{H[Zr_{12}Co_2O_8(OH)_{14}(pr)_{22}(MeCN)_2(\mu\text{-pz})][Zr_6Co_6O_8(pr)_{12}(Hbda)_6](NO_3)_3\cdot 8MeCN\}_n$ (**1**), in which clusters of both the $\{Co_6Zr_6\}$ and the $\{Co_2Zr_{12}\}$ types co-crystallize (H_2bda: *N*-butyldiethanolamine). Here, pyrazine (pz) selectively coordinates to the Co centers of the $\{Co_2Zr_{12}\}$ moieties and interlinks the latter into a one-dimensional coordination polymer; we note that while a few zirconium oxide-based MOFs characterized by single-crystal X-ray diffraction exist,[4] **1** represents the first structurally characterized heterometallic zirconium oxide-based coordination polymer. Importantly, replacing the pz linker with an alternative potential linker reagent, 4,4′-biphenol (H_2bph), under otherwise comparable reaction conditions results in the formation of crystals of only the discrete $\{Co_6Zr_6\}$-type cluster, isolated as $[Co_6Zr_6O_8(pr)_{12}(Hbda)_6](Hbph)_2\cdot(H_2bph)$ (**2**).

The crystal structure of compound **1** (space group *C*2/*c*) features two non-connected main constituents, the charge-neutral $[Zr_{12}Co_2O_8(OH)_{14}(pr)_{22}(MeCN)_2(\mu\text{-pz})]_n$ coordination polymer (**A**) and the discrete cluster cation $[Zr_6Co_6O_8(pr)_{12}(Hbda)_6]^{2+}$ (**B**), next to nitrate counteranions and acetonitrile solvate molecules (Fig. 1).

A comprises the rare $\{Zr_{12}O_{22}\}$ cluster core, in which two octahedral $\{Zr_6\}$ building blocks are directly condensed *via* six μ_2-hydroxo bridges, whereas most other known $\{Zr_{12}\}$-type structures comprise $\{Zr_6\}$ halves interlinked by four bidentate carboxylate bridges.[5] In **A**, all external coordination sites of the $\{Zr_{12}\}$ subunit are assumed by oxygen atoms of 20 propionate ligands, 16 of which bridge neighboring Zr sites, and four bridge Zr_2/Zr_3 and their symmetry equivalents to the Co(II) sites (Fig. 2). The Zr centers are 7- or 8-coordinated by four μ_3-O(H) or μ_2-OH atoms and three or four O donors from the carboxylate groups (Zr–O: 2.178(6)–2.28(1) Å). The protonation of the μ_2-OH groups interlinking the two $\{Zr_6\}$ halves can be deduced from longer Zr–O bond distances ranging from 2.139(8) to 2.159(7) Å, as well as from the presence of weak hydrogen bonds (2.91(2)–3.00(2) Å) to the NO_3^- anions. The $\{Zr_6(\mu\text{-O(H)})_8\}$ subunits consist of four μ_3-O, the atoms O4, O6, O8, and O10 (Zr–(μ_3-O): 2.050(7)–2.195(8) Å), as well as the four protonated μ_3-O atoms O5, O7, O9, and

[a] *Institute of Inorganic Chemistry, RWTH Aachen University, 52074 Aachen, Germany. E-mail: paul.koegerler@ac.rwth-aachen.de; Fax: +49 241 80 92642*
[b] *Ames Laboratory, Iowa State University, Ames, IA 50011, USA*

† Electronic supplementary information (ESI) available: Crystallographic details, additional structural plots, thermal stability studies. CCDC 931733 and 931734. For ESI and crystallographic data in CIF or other electronic format see DOI: 10.1039/c3ce41829d

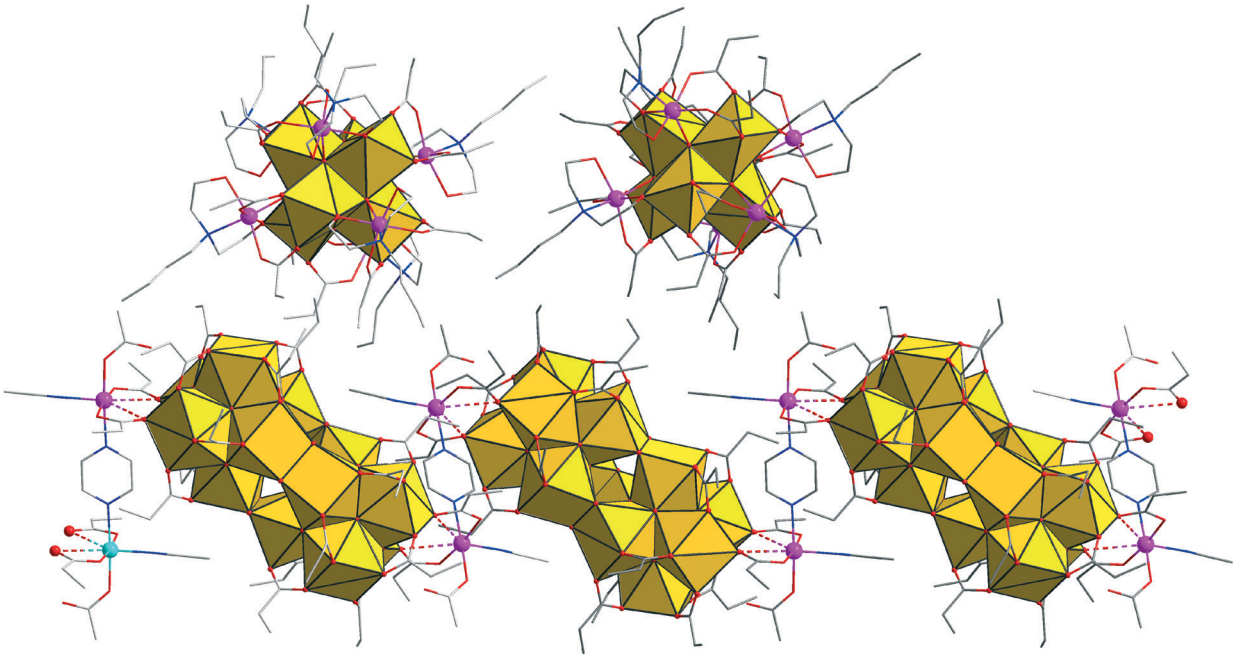

Fig. 1 A segment of the solid-state structure of **1** illustrating the coexistence of one helical polymer strand **A**, consisting of three pyrazine-linked $\{Co_2Zr_{12}\}$ groups, and two adjacent $\{Co_6Zr_6\}$ (**B**) clusters. The zirconium oxide substructures are shown in an octahedral representation. Co: purple spheres, C: grey, N: blue, O: red. Nitrate groups, acetonitrile solvate molecules, and hydrogen positions are omitted for clarity.

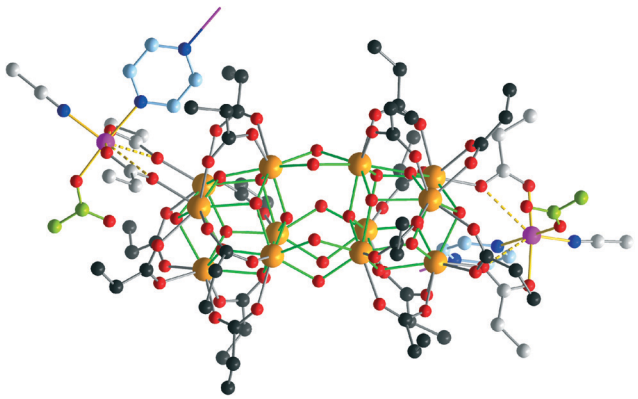

Fig. 2 The $\{Co_6Zr_{12}\}$ repetition unit in **A**. Green Zr–O bonds highlight the central zirconium oxide core. Zr: orange, Co: purple, O: red, N: dark blue spheres. C atoms, bidentate propionate groups: dark grey; pr groups bridging Zr and Co: light grey; monodentate pr: light green; pyrazine: light blue spheres. Solid yellow lines: Co–O/N coordinative bonds <2.1 Å; dashed yellow lines: weaker Co–O contacts (>2.7 Å). Hydrogen positions are omitted for clarity.

O11 (Zr–(μ_3-O): 2.360(6)–2.236(7) Å). The protonation of these atoms is also evident from the presence of hydrogen bonds to the monodentate carboxylates (2.70(1) Å) and to the nitrate groups (2.81(2) Å and 2.89(2) Å).

The two (crystallographically equivalent) Co(II) sites each coordinate to two oxygen atoms of two propionate ligands, and a pyrazine ligand coordinates to two adjacent Co sites of neighboring $\{Co_2Zr_{12}\}$ groups, resulting in an infinite helical chain (Fig. S1†). The square-prismatic CoN_2O_3 coordination environment includes one deprotonated terminal monodentate carboxylate displaying short C═O distances (1.20(2) Å), two bidentate carboxylates (Co–O_{carb}: 1.98(2)–2.07(1) Å), one MeCN and one pyrazine (Co–N: 2.11(1)–2.20(1) Å). The O sites of the bidentate pr groups binding to Zr form weak contacts with Co (Co–O: 2.72(1)/2.87(1) Å).

B features a $\{Zr_6(\mu_{3/4}\text{-O})_8\}$ core to which six additional Co atoms are attached *via* $Hbda^-$ groups to the μ_3-O sites. Chelating bda and carboxylate ligands connect the Co centers and adjacent Zr sites. The monodeprotonated $Hbda^-$ groups form intramolecular short hydrogen bonds (2.67(2)–2.68(1) Å) to neighboring carboxylate groups. Note that the $\{Zr_6(\mu_{3(4)}\text{-O})_8\}$ core in molecule **B** is not protonated as evident from the coordination of three μ_4-O (and their symmetry equivalents) to Co atoms and of one remaining μ_3-O (and its symmetry equivalent) to three zirconium atoms at distances of 2.081(8)–2.19(1) Å typical of Zr–(μ_3-O) bonds. The carboxylate ligands coordinate in $\mu_{1,2}$-bridging mode. The Co sites adopt a distorted octahedral NO_5 environment of two bidentate carboxylate ligands (Co–O_{carb}: 2.054(9)–2.10(1) Å) and one N (Co–N_{bda}: 2.17(1)–2.19(3) Å) and two O donors of a $bdaH^-$ ligand (Co–O_{bda}: 2.003(9)–2.09(1) Å), as well as one μ_4-O (2.118(8)–2.17(1) Å). The Zr sites are 7- or 8-coordinated by four $\mu_{3(4)}$-O atoms and three or four O donors from carboxylate and alkoxide groups (Zr–O: 2.079(8)–2.237(9) Å) (Fig. 3).

The NO_3^- groups in the crystal lattice of **1** are arranged around the bridging μ_2-OH groups that join the $\{Zr_6(\mu\text{-O(H)})_8\}$ subunits in **A**, thus forming a circular arrangement around the $\{Zr_{12}\}$ group (Fig. 4). Two of the three nitrates are symmetry equivalent with atom N10, while the third NO_3^- is

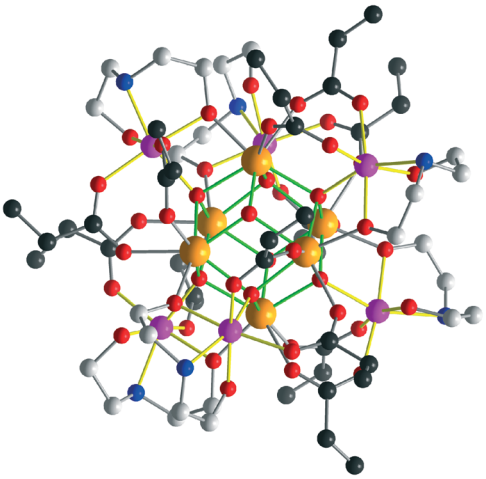

Fig. 3 Molecular structure of **B**. Color codes as in Fig. 2. The $\{Co_6Zr_6\}$ cluster in is virtually isostructural to **B**. Hydrogen and *n*Bu groups belonging to bda ligands are omitted for clarity.

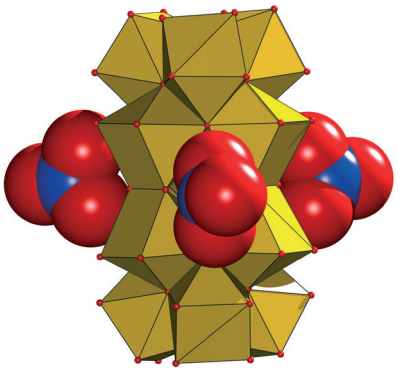

Fig. 4 Arrangement of the three nitrate groups (shown in their van der Waals spheres) around the $\{Zr_{12}\}$ core (in a polyhedral representation) in **1**.

crystallographically independent (N11), a potential indication for an interaction with an extra proton, which is required for the charge balance of complex **1**.

The crystal structure of compound **2** (space group $P6_322$) comprises the cationic cluster $[Zr_6Co_6O_8(pr)_{12}(Hbda)_6]^{2+}$, which is nearly identical to molecule **B** of compound **1** (see Fig. S2† for a comparison of the core geometries), and three 4,4′-biphenol groups per formula unit. As there is only one crystallographically unique biphenol group in the crystal lattice of **2**, charge balance requires it to formally be partly deprotonated ($H_{4/3}bph^{2/3-}$) on average. As in compound **1**, chelating bda and carboxylate ligands bind the Co centers and adjacent Zr sites. The bda alkoxide groups are monoprotonated and form intramolecular short hydrogen bonds (2.75(2) Å) to the neighboring carboxylate groups. As for **B**, the $\{Zr_6(\mu_{3/4}\text{-}O)_8\}$ core is also not protonated, and the indicative Zr–(μ_3-O) bonds measure 2.105(5)–2.189(9) Å. The NO_5-type Co coordination again shows typical geometrical parameters: $Co\text{–}O_{carb}$: 2.08(1)–2.08(2) Å, $Co\text{–}N_{bda}$: 2.19(1) Å, $Co\text{–}O_{bda}$: 2.02(1)–2.11(1) Å, and Co–(μ_4-O): 2.189(9) Å; the Zr–O bonds range from 2.105(5) to 2.23(1) Å.

Conclusions

The close similarity between the reaction conditions yielding compounds **1** and **2** highlights the sensitive nature of the equilibrium conditions under which different $\{Zr_6\}$ and $\{Zr_{12}\}$ zirconium oxide cluster archetypes can co-crystallize. We note that we, however, cannot rule out the co-existence of these cluster types in the reaction solution that eventually produces crystals of **2**: whereas the $\{Zr_{12}\}$ units in **1** are interlinked by pyrazine into a 1D coordination polymer, effectively reducing their solubility and facilitating precipitation, the 4,4′-biphenol linker employed in the reaction solution for compound **2** might simply be less affine to Co(II) coordination so as to adopt the same role. More systematic *in situ* studies of the reaction solutions are currently underway to determine how far the coexistence relations seen in the solid state relate to the conditions in the solution.

Notes and references

‡ See ESI† for the synthesis of $[Zr_6O_4(OH)_4(pr)_{12}]_2$·6Hpr precursors. Synthesis of $\{H[Zr_{12}Co_2O_8(OH)_{14}(pr)_{22}(MeCN)_2(pz)]\cdot[Zr_6Co_6O_8(pr)_{12}(Hbda)_6](NO_3)_3\cdot 8MeCN\}_n$ (**1**). A solution of 0.36 g (0.1 mmol) of $[Zr_6O_4(OH)_4(pr)_{12}]_2$·6Hpr (derived from $Zr(OBu)_4$),[5] *N*-butyldiethanolamine (0.085 mL, 0.51 mmol), 60 mg (0.2 mmol) of $Co(NO_3)_2\cdot 6H_2O$, and pyrazine (40 mg, 0.5 mmol) in 5 mL acetonitrile was refluxed for 1 h. Upon cooling to room temperature, the solution was kept in a parafilm-covered vial. Pink crystals of **1** were obtained after several days, washed with acetonitrile and dried in air (yield: 0.027 g). Elemental analysis, calcd. (found) for $C_{174}H_{327}Co_8N_{21}O_{119}Zr_{18}$: Co, 7.0 (6.14); C, 31.2 (32.25); H, 4.9 (3.04); N, 4.4 (4.75); Zr, 24.4 (26.4)%. IR data (KBr, ν/cm^{-1}): 3425 br/m, 2973 s, 2940 m, 1628 s, 1568 s, 1469 s, 1439 s, 1384 s, 1303 s, 1081 m, 1013 w, 906 w, 811 m, 632 s, 482 m, 414 w. Synthesis of $[Co_6Zr_6O_8(pr)_{12}(Hbda)_6](Hbph)_2\cdot(H_2bph)$ (**2**). A solution of 0.19 g (0.053 mmol) of $[Zr_6O_4(OH)_4(pr)_{12}]_2$·6Hpr (derived from $ZrCl_4$, see ESI†), *N*-butyldiethanolamine (0.085 mL, 0.51 mmol), 60 mg (0.2 mmol) of $Co(NO_3)_2\cdot 6H_2O$ and 90 mg (0.48 mmol) of 4,4′-biphenol was refluxed for 1 h in 5 mL of acetonitrile. Upon cooling to room temperature, the solution was kept in a parafilm-covered vial. Pink crystals of **1** formed after several days and were separated and washed with acetonitrile and dried in air (yield: 0.018 g). Elemental analysis, calcd. (found) for $C_{120}H_{196}Co_6N_6O_{50}Zr_6$: Co, 10.32 (9.16); C, 42.09 (42.29); H, 5.77 (5.65); N, 2.45 (2.49); Zr, 15.98 (15.6). IR data (KBr, ν/cm^{-1}): 3265 br/m, 2966 s, 1627 vs, 1502 s, 1467 m, 1438 m, 1302 mw, 1262 m, 1168 m, 1082 w, 904 m, 826 s, 619 w, 568 w, 542 w, 478 s. Single-crystal X-ray diffraction experiments were carried using a Bruker diffractometer with APEX II CCD detector with graphite monochromated MoKα radiation at a detector distance of 50.6 mm. Full-sphere data collection with exposures of 30 s per frame was made with ω scans in the range of 0–180° at φ = 0, 120, and 240°. A semi-empirical absorption correction was based on the fit of a spherical harmonic function to the empirical transmission surface as sampled by multiple equivalent measurements[6] using SADABS software.[7] Measurements were optimized to collect data to a resolution of 0.71 Å; however, the datasets have been truncated to obtain the statistically relevant resolution. The positions of metal atoms were found by direct methods. The remaining atoms were located in an alternating series of least-squares cycles and difference Fourier maps. All non-hydrogen atoms were refined in full-matrix anisotropic approximation. All hydrogen atoms were placed in the structure factor calculation at idealized positions and were allowed to ride on the neighboring atoms with relative isotropic displacement coefficients. **1**: $C_{174}H_{287}Co_8N_{21}O_{119}Zr_{18}$, monoclinic, $C2/c$, M_r = 6690.63 g mol^{-1}, T = 173(2) K, a = 36.819(4), b = 31.046(3), c = 28.384(5) Å, β = 123.688(1)°,

V = 26996(6) Å^3, Z = 4, 97 371 reflections, R_1 = 0.0752, wR_2 = 0.1916, R_1 (all data) = 0.1198, wR_2 (all data) = 0.2613; CCDC 931734. **2**: $C_{120}H_{180}Co_6N_6O_{50}Zr_6$, hexagonal, $P6_322$, M_r = 3407.6 g mol^{-1}, T = 173(2) K, a = 18.423(5), c = 26.934(7) Å, V = 7917(4) Å^3, Z = 2, 42 012 reflections, R_1 = 0.0850, wR_2 = 0.2102, R_1 (all data) = 0.0855, wR_2 (all data) = 0.2106; CCDC 931733.

1 I. L. Malaestean, M. Speldrich, A. Ellern, S. G. Baca and P. Kögerler, *Dalton Trans.*, 2011, **40**, 331; I. L. Malaestean, A. Ellern, S. Baca and P. Kögerler, *Chem. Commun.*, 2012, **48**, 1499; I. L. Malaestean, A. Ellern and P. Kögerler, *Eur. J. Inorg. Chem.*, 2013, 1635.

2 F. R. Kogler, M. Jupa, M. Puchberger and U. Schubert, *J. Mater. Chem.*, 2004, **14**, 3133; P. Piszczek, A. Radtke, A. Grodzicki, A. Wojtczak and J. Chojnacki, *Polyhedron*, 2007, **26**, 679.

3 P. Piszczek, A. Radtke, A. Wojtczak, T. Muzioł and J. Chojnacki, *Polyhedron*, 2009, **28**, 279; I. L. Malaestean, M. Kutluca, M. Speldrich, A. Ellern and P. Kögerler, *Inorg. Chim. Acta*, 2012, **380**, 72.

4 W. Morris, B. Volosskiy, S. Demir, F. Gándara, P. L. McGrier, H. Furukawa, D. Cascio, J. F. Stoddart and O. M. Yaghi, *Inorg. Chem.*, 2012, **51**, 6443.

5 M. Puchberger, F. E. Kogler, M. Jupa, S. Gross, H. Fric, G. Kickelbick and U. Schubert, *Eur. J. Inorg. Chem.*, 2006, 3283.

6 R. H. Blessing, *Acta Crystallogr., Sect. A: Found. Crystallogr.*, 1995, **51**, 33.

7 G. M. Sheldrick, *Acta Crystallogr., Sect. A: Found. Crystallogr.*, 2008, **64**, 112.

